Potentials of Digitally Sampling Scintillation Pulses in Timing Determination in PET

Journal:	*IEEE Transactions on Nuclear Science*
Manuscript ID:	TNS-00534-2008.R1
Manuscript Type:	Imaging and Instrumentation for Nuclear Medicine
Date Submitted by the Author:	n/a
Complete List of Authors:	Xie, Qingguo; Huazhong University of Science and Technology, Biomedical Engineering; Wuhan National Laboratory for Optoelectronics Kao, Chien-Min; The University of Chicago, Radiology Wang, Xi; Huazhong University of Science and Technology, Biomedical Engineering Guo, Ning; Huazhong University of Science and Technology, Biomedical Engineering Zhu, Caigang; Huazhong University of Science and Technology, Biomedical Engineering Frisch, Henry; The University of Chicago, HEP Moses, William; Lawrence Berkeley Lab Chen, Chin-Tu; The University of Chicago, Radiology
Standard Key Words:	PET, Digital signal processing, Scintillation detectors

(submitted to *IEEE Transactions on Nuclear Science*, 2008)

Potentials of Digitally Sampling Scintillation Pulses in Timing Determination in PET

Qingguo Xie, *Member, IEEE,* Chien-Min Kao, *Senior Member, IEEE,* Xi Wang, Ning Guo, Caigang Zhu, Henry Frisch, William W. Moses, *Fellow, IEEE,* and Chin-Tu Chen

***Abstract*—We investigate the potentials of digitally sampling scintillation pulses techniques for positron emission tomography (PET) in this paper, focusing on the determination of the event time. We have built, and continue building, a digital library of PET event waveforms generated with various combinations of photo-detectors and scintillator materials, with various crystal sizes. Events in this digital library are obtained at a high sampling of 20 GSps (Giga-samples per second) so that their waveforms are recorded with high accuracy. To explore the potential advantages of digitally sampling scintillation pulses, we employ a dataset in the above-mentioned library to evaluate two methods for digitizing the event pulses and linear interpolation techniques to analyze the resulting digital samples. Our results show that the two digitization methods that we studied can yield a coincidence timing resolution of about 300 ps FWHM when applied to events generated by a pair of LSO+PMT detector units. This timing resolution is comparable with that is achieved for the same detector pair with a constant fraction discriminator. As a benchmark, regular-time sampling (RTS) method, usually implemented with very fast traditional analog-to-digital converters (ADCs) for digitizing scintillation pulses is not feasible for a multi-channel system like a PET system. Digitizing scintillation pulses with multi-voltage threshold (MVT) method could be implemented at a reasonable cost for a PET system. With digitized PET event samples, various digital signal processing (DSP) techniques can be implemented to determine event arrival time. Our results have therefore demonstrated the promising potential of digitally sampling scintillation pulses techniques in PET imaging.**

***Index Terms*—Positron Emission Tomography (PET), Digital Signal Processing (DSP), Scintillation Pulse**

I. Introduction

THE electronics technology is undergoing digital revolution and the strengths of digital signal processing (DSP) in consumer electronics are well established. In biomedical imaging, the advantages of using DSP technologies have been demonstrated in ultrasound imaging and magnetic resonance imaging (MRI) [1], [2]. DSP approaches have also been successfully used to improve the energy resolution and reduce the dead time in γ-ray and X-ray detectors [3]. In modern positron emission tomography (PET), some forms of digital data-acquisition (DAQ) have been implemented. Generally, for LSO crystals the event pulses are shaped and then digitized by use of $\sim$20-200 MSps (Mega-samples per second) analog-to-digital converters (ADCs) to obtain only $\sim$40 samples per event [4]–[6]. The small number of digital samples obtained for an event is primarily used for improving the energy resolution, handling event pileup and baseline shifting, and reducing the dead time [6]. For determining the event time, digital constant fraction discriminator (CFD) and leading-edge triggering have been considered [7], [8], but the use of analog CFDs is still common. The typical coincidence timing resolution of modern PET systems is in the range of $\sim$1 ns to $\sim$4 ns. For time-of-flight (TOF) PET systems, $\sim$570 picosecond (ps) coincidence timing resolutions are reported [9], [10]. Therefore, PET event processing still follows the general principle that is developed decades ago with analog devices [11], [12]. Also, analog circuit blocks, such as shaper amplifier or CFDs, are still involved in PET event processing as key components.

Digitizing PET event pulses to capture their waveforms and applying digital-signal analysis to the resulting samples for generating relevant event information enable eliminating analog circuit blocks as much as possible. The development of such DAQ schemes for PET has both theoretical interest and practical significance. Successful development of PET digital DAQ by minimizing analog circuit blocks will enable PET scientists to tap into the large collection of general-purpose digital electronics components available in the market and the large amount of resources existing to support these components. It also allows one to reap the benefits of the continuous and aggressive technological inventions and upgrades that are driven by the vast interest in the DSP technology from almost every areas of consumer electronics. As a result, the development of digitally sampling scintillation pulses technology can bring about faster upgrade and lower cost [13], [14]. Another benefit is related to the capability to easily test and implement various event-processing algorithms for generating more accurate energy, timing and position information about an PET event. PET DAQs with digital pulse processing by use of shapers and moderate sampling rate ADCs have been proposed and demonstrated [5], [7], [15]. In this paper, we present our initial efforts in exploring and revealing the possible advantages

Qingguo Xie is with the Biomedical Engineering Department, Huazhong University of Science and Technology, Wuhan, Hubei, China and also with the Wuhan National Laboratory for Optoelectronics, Wuhan, Hubei, China. E-mail:qgxie@ieee.org

Chien-Min Kao is with the Department of Radiology, The University of Chicago, Chicago, IL, USA

Xi Wang, Ning Guo, and Caigang Zhu are with Biomedical Engineering Department, Huazhong University of Science and Technology, Wuhan, Hubei, China

Henry Frisch is with the Enrico Fermi Institute, The University of Chicago, Chicago, IL, USA

William W. Moses is with the Lawrence Berkeley National Laboratory, Berkeley, California, USA

Chin-Tu Chen is with the Department of Radiology, The University of Chicago, Chicago, IL, USA

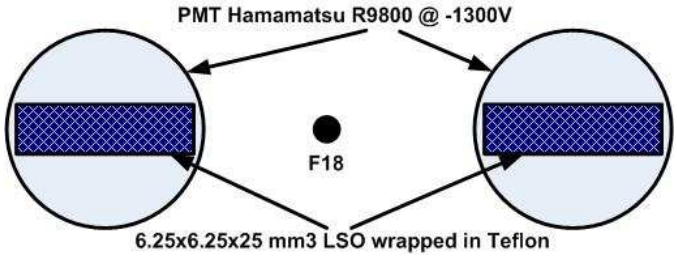

Fig. 1. Experimental setup for producing a digital library of PET events

of processing PET events digitally. We build digital pulse libraries for PET that would enable us to effectively study and compare different analysis methods. Therefore, we employ such libraries to investigate the baseline performance of two digital sampling and analysis methods that do not consider the noise characteristics of the samples. In general, the bias and the variance of an estimate decrease with increasing number of observation samples [16] [17]. The two methods include one method that generates multiple samples at pre-defined voltage thresholds and another method that generates multiple samples at regular time intervals. Digital samples generated by both methods for an event are fitted with a straight line to determine the event time. First, we evaluate whether digitizing PET event waveforms at a sufficiently high sampling rate can bring out any advantages in terms of improving event timing. Second, to mitigate the practical challenge in using high-speed ADC we investigate the multi-voltage threshold sampling method as an alternative to the conventional sampling method. We focus on the task of event-time determination, with an interest in examining the possibility of achieving reasonable timing resolution for TOF-PET imaging.

II. Digital Library of PET Event Pulses

Figure 1 illustrates the experimental setup for producing the digitized event waveforms for evaluating various digitization schemes and DSP methods. The LSO crystals, of $6.25 \times 6.25 \times 25\,\mathrm{mm}^3$ in size, are optically coupled to the Hamamatsu R9800 photomultiplier tubes (PMTs) via one of their $6.25 \times 25\,\mathrm{mm}^2$ surfaces, with the other five surfaces wrapped in Teflon tape. The PMTs are operated at -1300 Volt and their outputs are directly connected to a Tektronics TDS6154C digital storage oscilloscope with a $50\ \Omega$ termination. This scope has a 15 GHz bandwidth and provides a sampling rate up to 40 GSps. When performing simultaneous sampling on two channels, its sampling rate becomes 20 GSps per channel (i.e., a 50 ps sampling interval). A weak F-18 source is placed at a location close to one of the LSO/PMT unit. The scope is then triggered by an event generated at the far-side LSO/PMT unit, thereby ensuring that the majority of the recorded event pairs are coincidence events. For each recorded event pair, 4000 samples from each channel are generated. Therefore, the pulses are recorded for a duration of 200 ns, which is adequate with respect to the $\sim$40 ns scintillation decay of the LSO.

Figure 2 shows a sample pair of digitized event pulses. Event energy is estimated by summing up all the digitized samples of a pulse. Figure 3 shows the resulting pulse-height spectrum, calibrated to 511 keV, derived from a dataset

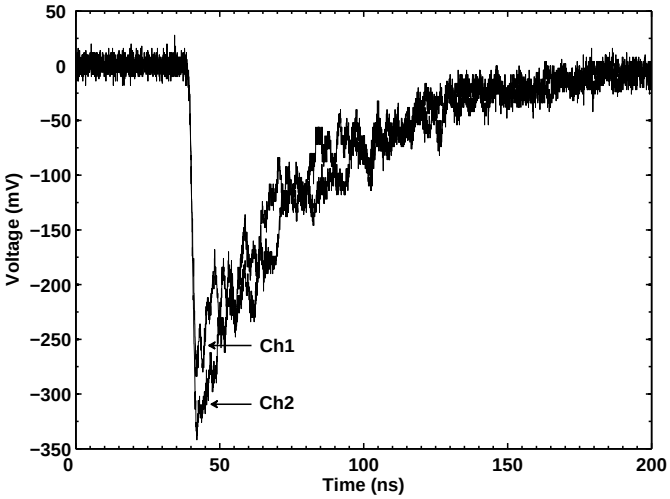

Fig. 2. A sample digitized event pair. The events are sampled by a Tektronics TDS6154C digital scope at a 50 ps interval. Each record contains 4000 samples per channel.

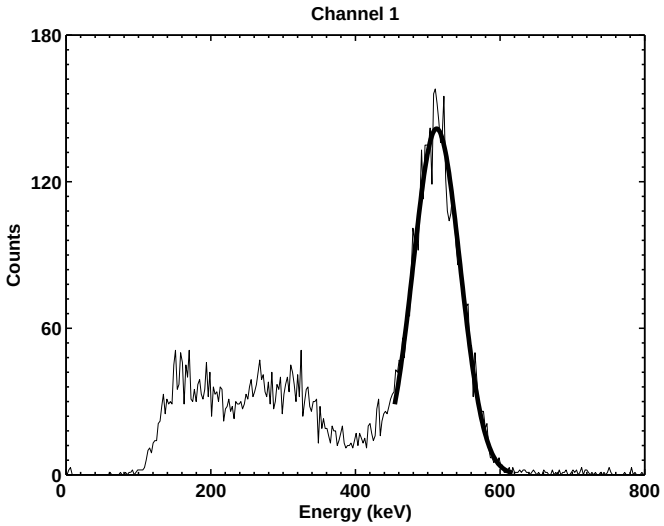

Fig. 3. The energy histogram obtained from a dataset containing 9000 event pairs. Only the histogram obtained for events acquired at the channel 1 of the digital scope is shown. A Gaussian fit to the photopeak (thick black curves) indicates an energy resolution of about 16% FWHM.

containing a total of 9000 event pairs. A Gaussian fit to the photopeak indicates an energy resolution of 16.0% FWHM at 511 keV for events acquired at channel 1 of the scope. Similarly, the event acquired at channel 2 has an energy resolution of 14.3% at 511 keV (data no shown). Figure 4 shows the mean and variance of the digitized pulses having energy in the range of 511 ± 25.5 keV. The mean pulses show a rising time of 1.7 ns. Also, the exponential decay constant is 41.0 ns, which is consistent with the value reported in the literature for LSO [18]. For these pulses, we also calculate the amplitude-frequency response for every pulse by using of fast Fourier transform (FFT), and then average to obtain the mean and variance (see Fig. 4e and Fig. 4f).

In addition to the LSO/PMT detectors described above, our pulse library also contain digitized events generated by other scintillators and photo-detectors (PDs). Our library also

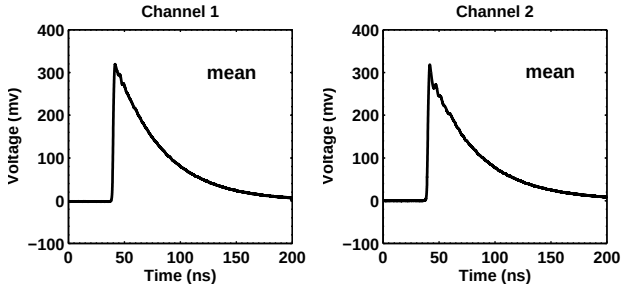

(a) Means of the acquired pulses

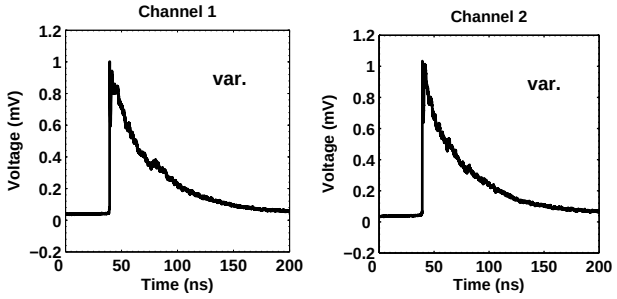

(b) Variances of the acquired pulses

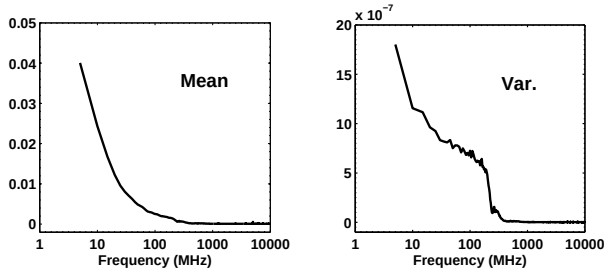

(c) Means (left) and variances (right) of the acquired pulses for channel 2 in the frequency domain.

Fig. 4. Means and variances of the acquired pulses in the 511 ± 25.5 keV energy in both time and frequency domains.

contains events generated by the HRRT (High Resolution Research Tomograph) detector modules [19]. The HRRT detector modules contains an 8×8 array of double-layered LSO/LYSO crystals, coupled to a 2×2 PMT array in a quadrant-sharing configuration. Individual crystal segment of the detector module is $2.1 \times 2.1 \times 10\,\text{mm}^3$ in size. The LSO and LYSO are different in their scintillation light decay time constants. Therefore, the DAQ electronics can determine inside which crystal a detected event is generated based on the scintillator decay. This library is very valuable for testing different pulse digitization schemes and DSP methods, and comparing their performance in terms of various event information of interest such as event time, event energy, crystal identification in a block detector, and depth-of-interaction resolution.

III. Coincidence timing resolution with CFD

The conventional analog CFD is a well-established and widely-used technique for PET event-time determination. Figure 5 shows the coincidence timing histograms of the

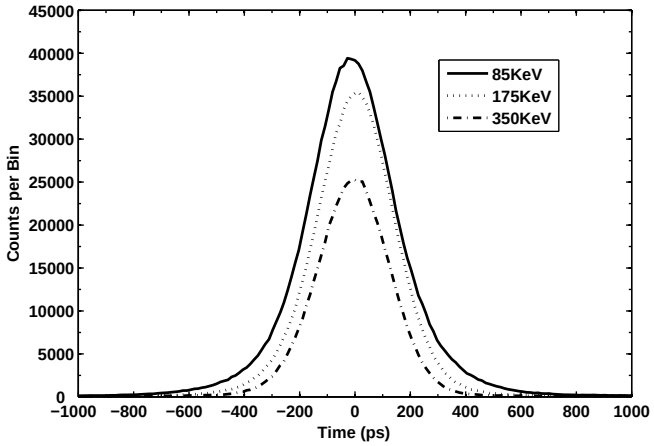

Fig. 5. Coincidence timing histograms of the LSO/PMT modules shown in Fig. 1, measured by using a Canberra 454 fast CFD with three energy thresholds. An coincidence timing resolution of about 300 ps FWHM is obtained.

LSO/PMT modules measured by use of the Canberra 454 fast CFD (attenuation=0.2, delay=1.6ns). We obtain a coincidence timing resolution of 297 ps, 313 ps, and 314 ps full-width-at-the-half-maximum (FWHM) when using 350, 175, and 85 keV thresholds for the CFD, respectively.

Our CFD results are measured by using the Canberra 454 fast CFD, taking analog signals directly from PMT outputs. On the other hand, our results obtained for the two digitizing methods (in Sect. IV) are derived from pulse library containing sampled waveforms. By implementing a SPICE model for the CFD (see Fig. 6) and applying it to the LSO/PMT dataset containing 9000 event pairs as described above in Sect. II, we provide evidence that validate the use the 20 GSps digital sampling library. Figure 7 shows the coincidence time histograms obtained by using a 0.2 attenuation and 1.6 ns delay in the CFD model. These histograms show a coincidence timing resolution of 314 ± 12 ps, 356 ± 8 ps, and 403 ± 13 ps FWHM when using 350, 175, and 85 keV thresholds for the software CFD. Other attenuation and delay settings are also examined. Table I summarizes the coincidence timing resolution obtained with a 350 keV threshold. We observe a coincidence timing resolution of $\sim$300 ps. This agreement with the Canberra 454 CFD results indicates that we can use the 300 ps timing resolution obtained by use of the fast analog CFD as a benchmark for evaluating the digital event-time determination methods that we will describe below.

IV. Digital methods for event-time determination

We study two digital techniques for determining the event time. For testing these methods, we only select the events in our dataset having energies above 350 keV. We obtain a total of 3579 event pairs when applying this selection. The two techniques of interest differ in their schemes for digitizing the event waveforms. The development of adequate DSP methods for generating the most accurate event-time estimate may require carefully statistical characterizations of

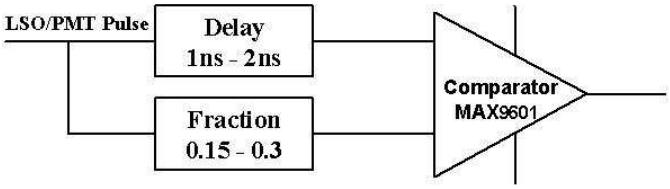

Fig. 6. The SPICE CFD model. The LSO/PMT input pulses are derived from the digitized event waveforms generated as described in Sect. II. The attenuation and delay settings of the model can assumed the ranges of values as indicated.

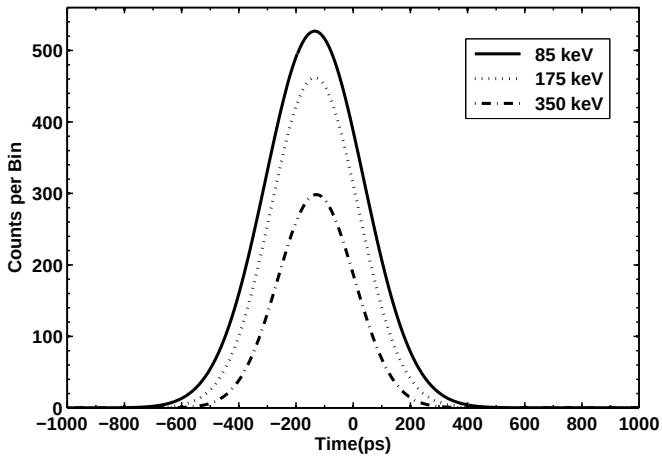

Fig. 7. Gaussian fits to coincidence timing histograms by use of the SPICE CFD model (0.2 attenuation and 1.6 ns delay), with three energy thresholds. The bin size is 50 ps Their FHWMs range from 314 ps to 430 ps, which is similar to but slightly worse than those obtained by actual measurements shown in Fig. 5 by using a Canberra 454 CFD.

TABLE I
COINCIDENCE TIMING RESOLUTIONS BY USE OF A SPICE CFD MODEL AND AN LSO/PMT DATASET IN OUR DIGITAL PULSE LIBRARY.

atten	delay (ns)	FWHM
0.15	1.0	323 ± 11 ps
0.20	1.0	306 ± 6 ps
0.30	1.0	314 ± 9 ps
0.15	1.6	302 ± 10 ps
0.20	1.6	314 ± 12 ps
0.30	1.6	344 ± 8 ps
0.15	2.0	302 ± 10 ps
0.20	2.0	310 ± 11 ps
0.30	2.0	352 ± 15 ps

the noise properties of the pulse and employ them in statistics-based estimation approaches [4]. In this paper, we examine the use of linear regressions to the samples obtained on the leading edges of the event pulses for generating estimates for the event time. The RMS noise of the oscilloscope and PMT derived from the saved waveforms is 9.0 mV. We observe that the $\sim 15\%$-$\sim 75\%$ is quite linear. In this paper, we only use a straight line to fit the digitized samples. We suspect that timing resolution may be improved by spreading the samples, either reference voltages or regular time samples to the linear part of rising edges.

A. Multi-voltage threshold (MVT) method

This method is a modification of the technique that we previously reported in [13]. In this method, samples of an event pulse with respect to a number of pre-defined voltage references are obtained (see Fig. 8). In practice, this digitizing scheme can be implemented by use of a number of discriminators having programmable thresholds. The LSO/PMT output feeds directly to these discriminators and the time when the leading edge of the discriminator output occurs can be determined by use of a time-to-digital converter (TDC). With this method, the resulting digital samples are generated at irregular time intervals depending on the characteristic shape of the event waveform. As long as the thresholds are properly defined with respect to the energy values of the events of concern, a fixed number of digital samples can be generated for the leading edge of the event pulse, regardless of how short the event rising time is. This is in contrast to the conventional ADC scheme to be discussed below in Sect. IV.B.

The event waveforms in our dataset are sampled at a 50 ps interval. This fine sampling allows us to accurately reproduce the waveforms by linearly interpolating the samples and emulate the MVT digitizing scheme by mathematically determining the time points when a waveform cross the pre-defined voltages. After obtaining the digital samples, we fit them with a regression line and estimate the event time by the intercept of this line with the zero-voltage baseline. Figure 8(b) illustrates the use of four thresholds on an event pulse, along with the linear-regression line to the resulting samples. Here, the reference voltages are defined by[1]

$$V_n = g(V_{ST} + 150n/N) \ \text{mV}, n = 0, \cdots, N-1, \quad (1)$$

where N is the number of thresholds, $V_{ST} = 40$ is the lowest threshold, and g is a positive number. The value of g is used to account for the difference in the gains of the two acquisition channels. We use $g = 0.81$ and 1 for channels 1 and 2, respectively. Figure 9 shows the coincidence timing histogram obtained by use of these four voltage thresholds and the LSO/PMT events having energies above 350 keV in our dataset. By fitting the histograms with Gaussian functions, we obtain coincidence timing resolutions of 353 ± 11 ps, 330 ± 10 ps, and 318 ± 10 ps FWHM when using 4, 6, and 8 voltage thresholds, respectively. The coincidence timing resolution obtained with the use of 8 thresholds corresponds to a standard deviation of about 95 ps for single channel.

We also study the use of the following reference voltages:

$$V_n = V_{ST} + n \times V_{TS} \ \text{mV}, n = 0, 1, \cdots, N-1 \quad (2)$$

[1]We note that the average peak amplitude of the pulses having energies in the range of 350 ± 17.5 keV is 244 mV. We spread the reference voltages to 15% - 75% rising edge of LSO/PMT pulses. Hence, the spaced voltage of 150 mV is determined.

where N is the number of thresholds, V_{ST} is the lowest threshold and V_{TS} is the voltage step. We allow N, V_{ST} and V_{TS} to be variable and investigate how the coincidence timing resolution varies with these parameters. Figure 10 shows the timing resolution obtained with four thresholds, three settings for V_{ST}, and various V_{TS} ranging from 10 mV to 55 mV. It is observed that the timing resolution improves to reach a FWHM of ∼350 ps as the V_{TS} increases. It also shows that the best timing resolution is obtained by using V_{ST} approximately equal to 40 mV. Figure 11, on the other hand, shows the variation of the timing resolution with the number of thresholds, with the reference voltages defined by Eq. (1) and $V_{ST} = 40$ mV. It is observed that the resolution improves considerably as the number of threshold increases from 2 to about 8. It implies that multiple time pick-offs, spaced in voltage, could improve timing information by averaging noisy data. Adding more thresholds after that yields only marginal improvements and therefore may not be cost effective. The coincidence timing resolutions obtained are 370 ps, 350 ps and 320 ps FWHM when using 2, 4, and 8 thresholds. The best timing resolution achievable for this LSO/PMT dataset is about 302 ± 8 ps FWHM by use of 16 thresholds, which is consistent with the result obtained by use of the SPICE CFD. We also obtain timing resolutions of 355 ps, 388 ps, and 537 ps FWHM by use of leading edge discriminators (LED) with thresholds of 40 mV, 115 mV, and 190 mV, respectively.

We note that the timing resolution reported above contain the timing uncertainties of the scope and those are due to the use of the 50 ps sampling interval. In addition, we have somewhat arbitrarily considered the use of regularly spaced thresholds. To achieve the best timing resolution, the thresholds need to be selected according to the temporal characteristics of the event pulse and also the statistical properties of the noise. Our results have nevertheless demonstrated the capability of the MVT method to generate a good coincidence timing resolution for TOF-PET imaging.

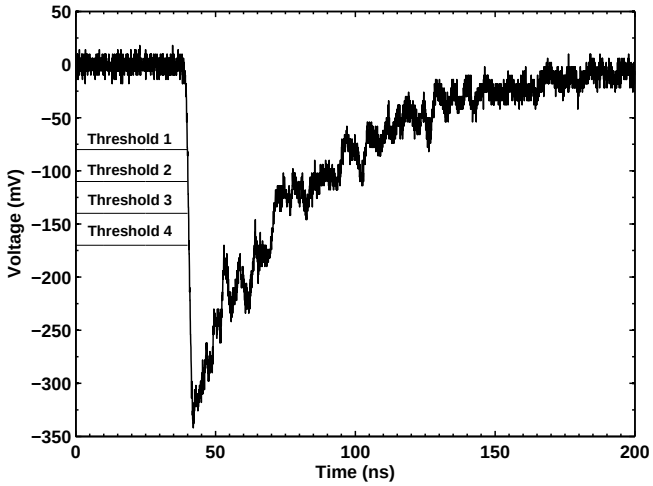

(a) Four thresholds applied an event pulse.

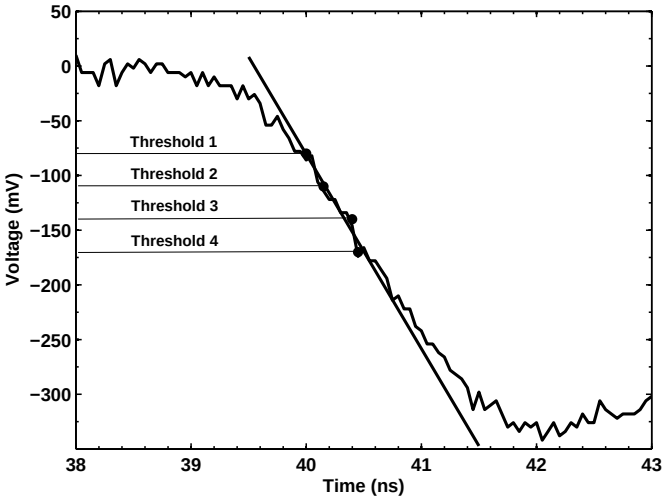

(b) Linear fitting to the digital samples obtained by applying the four thresholds.

Fig. 8. The 4-threshold MVT method applied to a sample event pulse. The event time is defined by the intercept of the linear regression line with the zero-voltage baseline.

B. Regular-time sampling (RTS) method

The RTS method adopts the conventional ADC scheme for digitization, i.e., it generates digital samples of event pulses at regular time intervals. The ADC is the core component of digital electronics. It is readily available; significant improvements to its sampling rate are being continually made; and its cost is rapidly decreasing. This digitizing scheme, therefore, has the advantages of receiving the widest community support. One important consideration of using RTS is the sampling rate. With a low sampling rate, the leading edge of the event pulse will not be properly sampled (or missed entirely), hence an inaccurate event time will be generated. On the other hand, cost becomes a concern if a high sampling rate is required to accurately catch the transient behavior of the event pulse.

We study the timing accuracy that can be achieved by use of the RTS method at various sampling rates that are emulated by properly sub-sampling the event waveforms obtained at 20 GSps. In sub-sampling, the data points inside a sub-sample interval are averages for implementing the 'S/H' operation in ADC. As a result, we note that the signal-to-noise ratio (SNR) of the sampled event pulse increases as the sampling rate decreases. Again, the development of DSP methods for optimally analyzing the resulting samples is an open research area. In this paper, we will consider the use of the linear regression method as described above for the MVT method. Figure 12 illustrates the application of the RTS sampling scheme, at 6.67 GSps, to an event pulse and the linear regression fitting to the resulting samples above a 40 mV threshold. Figure 13 shows the resulting coincidence timing histogram at this sampling rate, which indicates a coincidence timing resolution of 299 ± 8 ps FWHM. It implies that multiple time pick-offs, spaced in time, could improve the timing resolution by averaging the fluctuation of scintillation pulse samples. Similarly, we obtain a coincidence timing resolution of 335 ± 10 ps, 322 ± 11 ps, 298 ± 8 ps and 294 ± 8 ps when using the a sampling rate of 2.85 GSps, 3.33 GSps, 10.0 GSps

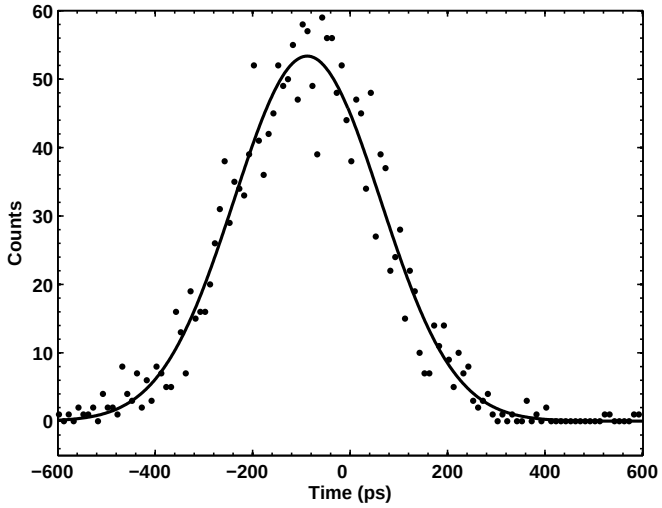

Fig. 9. The coincidence timing histogram obtained by the MVT method with four thresholds equal to 40, 90, 140, 190 mV. The thick curve is the Gaussian-fitting curve; it has a FWHM of ∼353 ps.

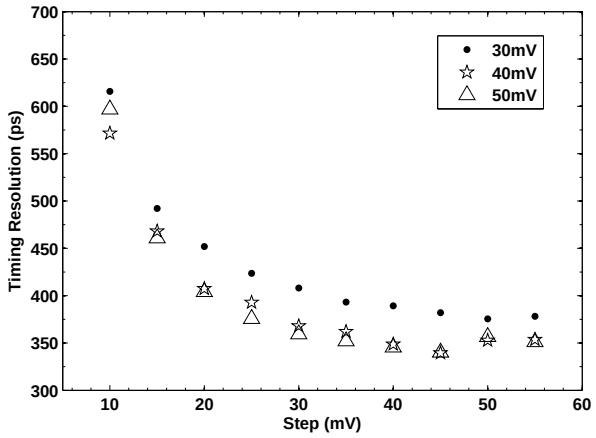

Fig. 10. Dependence of the coincidence timing resolution on the step of the reference voltages. We consider the use of four thresholds. The lowest thresholds are either 30, 40, or 50 mV. See Eq. (2) for definition.

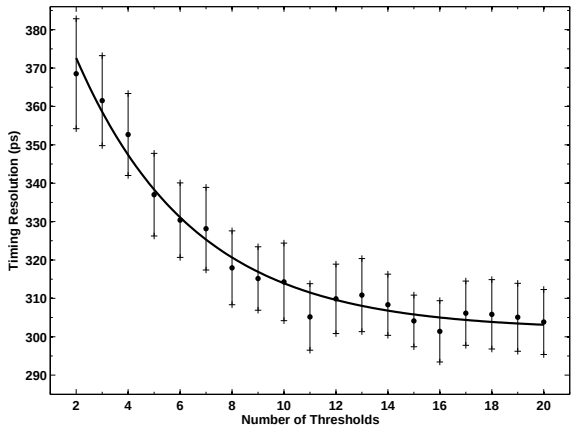

Fig. 11. Dependence of the coincidence timing resolution on the number of voltage threshold. See Eq. (1) for definition.

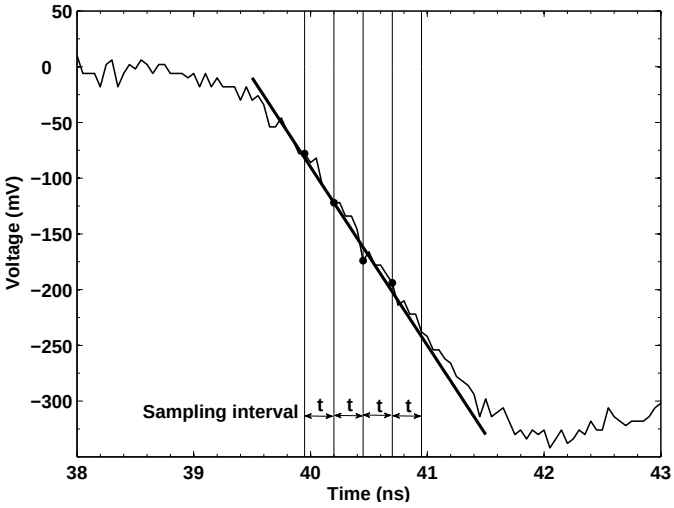

Fig. 12. The RTS method applied to a pulse event. The sampling rate is 6.67 GSps and the thick black line shows the linear regression line through the samples obtained at the leading edge of the pulse.

and 20.0 GSps[2], respectively (see Fig. 14). The RTS method breaks at a lower sampling rate than 2.5 GSps. The event time of only $\sim 55\%$ and $\sim 10\%$ pulses can be extracted at 2.5 GSps and 2.0 GSps sampling rate, respectively. Therefore, to provide a 320 ps coincidence timing resolution, a sampling rate above 3.33 GSps is needed [17]. We note that we obtained about 3 samples on the leading edge of the LSO/PMT pulses at a 3.33 GSps sampling rate.

V. Conclusion

We have built a substantial library of digitized waveforms obtained at a high sampling rate of 20 GSps, of event pairs generated in PET imaging. The library currently contains events generated by a pair of LSO/PMT detectors, a pair of LYSO/MPPC detectors, and a pair of the HRRT detector modules. We are extending our library to include more combinations of photo-detectors and scintillators, as well as different readout electronics. We have employed a dataset in this library that contains 9000 pairs of events generated by the LSO/PMT detectors to study two digital methods for determining the event time in PET. We show that these methods can all achieve a coincidence timing resolution of ∼300 ps FWHM, which is comparable with that obtained by use of a fast analog CFD and is adequate for TOF-PET imaging. In real-world practice, the RTS method implemented with ADCs is not feasible at present due to a high sample rate requirement. Also, a buffer amplifier is still required for full use of an ADC's dynamic range. Also, CFDs are very hard to implement in ASICs because of the need for a high frequency analog delay line, while leading edge discriminators and TDCs are relatively easily implemented. Exactly for mitigating the practical challenge in

[2]We naturally choose $\frac{1}{2}$, $\frac{1}{3}$, $\frac{1}{4}$, ..., etc of 20 GSps to subsample pulses acquired by the 20 GSps scope.

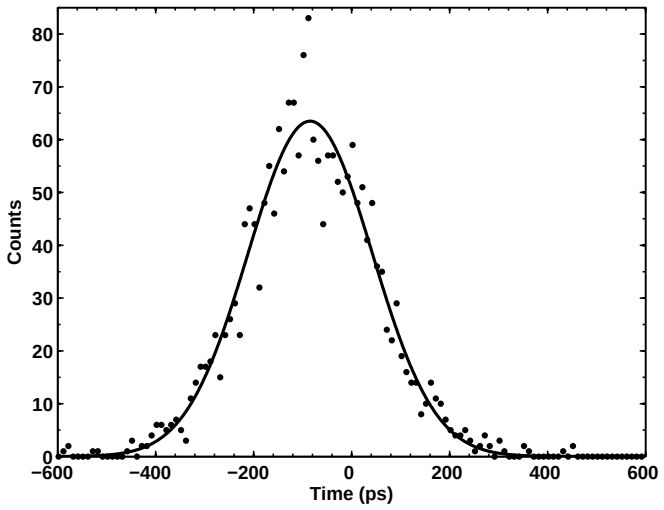

Fig. 13. The coincidence timing histogram obtained by use of the RTS method at the 6.67 GSps sampling rate. The Gaussian fit yields a coincidence timing resolution of about 300 ps FWHM.

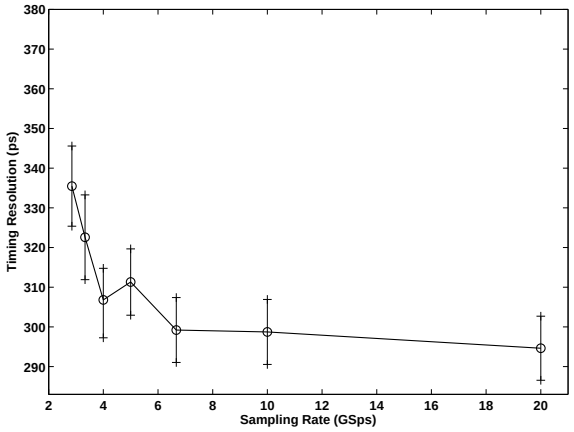

Fig. 14. Sampling rate dependence of coincidence timing resolution

using high-speed ADC we have investigated the MVT method as an alternative to the conventional sampling method. Our encouraging results are obtained by using the two methods that do not model noise properties and assume a simple linear leading-edge for the event pulse. We believe that better results may be obtained if the characteristics of the pulse and noise are modeled and employed in the event time determination. In this paper, we have focused on determining the event time. Once digital samples of the pulses are available, other event information, such as the energy and decay constant, can also be derived by analyzing these samples with proper algorithms. With modern technology, sophisticated DSP techniques can be readily implemented by using high-density FPGAs. We notice that results reported in this paper are obtained by directly sampling the LSO/PMT output, without using pre-amplifiers and shapers. Therefore, the resulting digital DAQ architecture can be quite simple and is entirely free of analog electronics components.

ACKNOWLEDGMENT

The authors thank Gary Drake and John Anderson for making the digital scope available to this research and assisting in the experimental setup. We also thank Qian Zhang, Shuijin Su, and Zheng Tian for their excellent technical help and discussion. We appreciate Patrick LeDu, Christophe Royon, Na Li, Bo Zhang, Octavia Biris, Jialie Lin and Dan Herbst for helpful discussion. The scope was supported by a UChicago Argonne internal grant, LDRD #2006-075-NO. This work was also supported in part by the ACS-IRG grant #6-9512, the NIH grants R01 EB000225, R33 EB001928, and R01 EB006085, the NSF grant PHY04-5668, the DOE grant DE FG02-06 ER 41426, the NSF (China) grant #60602028, the Ministry of Science and Technology (China) grant #2006AA02Z333, and the Ministry of Education (China) grant #107073. The Argonne and Lawrence Berkeley National Laboratories are supported by the Office of Science of the Department of Energy under contract number DE-AC02-06CH11357 and DE-AC02-05CH11231.

REFERENCES

[1] N. Rao and S. Mehra, “Medical ultrasound imaging using pulse compression,” *Electronics Letters*, vol. 29, pp. 649–651, 1993.

[2] P. N. Morgan, R. J. Iannuzzelli, F. H. Epstein, and R. S. Balaban, “Real-time cardiac mri using dsps,” *Medical Imaging, IEEE Transactions on*, vol. 18, pp. 649–653, 1999.

[3] H. Tan, T. A. DeVol, and R. A. Fjeld, “Digital alpha/beta pulse shape discrimination of csi:tl for on-line measurement of aqueous radioactivity,” *Nuclear Science, IEEE Transactions on*, vol. 47, pp. 1516–1521, 2000.

[4] J. M. Cardoso, J. B. Simoes, C. M. B. A. Correia, A. Combo, R. Pereira, J. Sousa, N. Cruz, P. Carvalho, and C. A. F. Varandas, “A high performance reconfigurable hardware platform for digital pulse processing,” *Nuclear Science, IEEE Transactions on*, vol. 51, pp. 921–925, 2004.

[5] R. Fontaine, M. A. Tetrault, F. Belanger, N. Viscogliosi, R. Himmich, J. B. Michaud, S. Robert, J. D. Leroux, H. Semmaoui, P. Berard, J. Cadorette, C. M. Pepin, and R. Lecomte, “Real time digital signal processing implementation for an apd-based pet scanner with phoswich detectors,” *Nuclear Science, IEEE Transactions on*, vol. 53, pp. 784–788, 2006.

[6] A. Fallu-Labruyere, H. Tan, W. Hennig, and W. K. Warburton, “Time resolution studies using digital constant fraction discrimination,” *Nuclear Instruments and Methods in Physics Research Section A: Accelerators, Spectrometers, Detectors and Associated Equipment*, vol. 579, pp. 247–251, Aug 2007. [Online]. Available: http://www.sciencedirect.com/science/article/B6TJM-4NF4DY6-J/2/ea61d8c3ef1320eae44bd0c82fb59df8

[7] P. D. Olcott, A. Fallu-Labruyere, F. Habte, C. S. Levin, and W. K. Warburton, “A high speed fully digital data acquisition system for positron emission tomography,” in *Nuclear Science Symposium Conference Record, 2006. IEEE*, vol. 3, 2006, pp. 1909–1911.

[8] L. Arnold, R. Baumann, E. Chambit, M. Filliger, C. Fuchs, C. Kieber, D. Klein, P. Medina, C. Parisel, M. A. . R. M. Richer, C. A. . S. C. Santos, and C. A. . W. C. Weber, “Tnt digital pulse processor,” *Nuclear Science, IEEE Transactions on*, vol. 53, pp. 723–728, 2006.

[9] S. Surti, A. Kuhn, M. E. Werner, A. E. Perkins, J. Kolthammer, and J. S. Karp, “Performance of philips gemini tf pet/ct scanner with special consideration for its time-of-flight imaging capabilities,” *The Journal of Nuclear Medicine*, vol. 48, pp. 471–480, 2007.

[10] R. F. Muzic and J. A. Kolthammer, “Pet performance of the gemini tf: A time-of-flight pet/ct scanner,” in *Nuclear Science Symposium Conference Record, 2006. IEEE*, vol. 3, 2006, pp. 1940–1944.

[11] D. F. Newport and J. W. Young, “An asic implementation of digital front-end electronics for a high resolution pet scanner,” *Nuclear Science, IEEE Transactions on*, vol. 40, pp. 1017–1019, 1993.

[12] J. W. Young, J. C. Moyers, and M. Lenox, “Fpga based front-end electronics for a high resolution pet scanner,” *Nuclear Science, IEEE Transactions on*, vol. 47, pp. 1676–1680, 2000.

[13] Q. Xie, C. M. Kao, Z. Hsiau, and C. T. Chen, "A new approach for pulse processing in positron emission tomography," *Nuclear Science, IEEE Transactions on*, vol. 52, pp. 988–995, 2005.

[14] H. Li, W.-H. Wong, H. Baghaei, J. Uribe, Y. Wang, Y. Zhang, S. Kim, R. Ramirez, J. Liu, and S. Liu, "The engineering and initial results of a transformable low-cost high-resolution pet camera," *Nuclear Science, IEEE Transactions on*, vol. 54, pp. 1583–1588, 2007.

[15] A. R. McFarland, S. Siegel, D. F. Newport, R. Mintzer, B. Atkins, and M. Lenox, "Continuously sampled digital pulse processing for inveon small animal pet scanner," in *Nuclear Science Symposium Conference Record, 2007. NSS '07. IEEE*, vol. 6, 2007, pp. 4262–4265.

[16] S. V. Vaseghi, *Advanced Digital Signal Processing and Noise Reduction*, 2nd ed. New York, USA: John Wiley and Sons, Ltd., 2000.

[17] T. L. Folyd, *Digital Fundamentals*, 9th ed., Y. Qiu, Ed. Beijing, China: Publishing House of Electronics Industry, June 2006.

[18] C. L. Melcher, M. A. Spurrier, L. Eriksson, M. Eriksson, M. Schmand, G. Givens, R. Terry, T. Homant, and R. Nutt, "Advances in the scintillation performance of lso:ce single crystals," *Nuclear Science, IEEE Transactions on*, vol. 50, pp. 762–766, 2003.

[19] M. Rodriguez, J.-S. Liow, S. Thada, M. Sibomana, S. Chelikani, T. Mulnix, C. A. Johnson, C. Michel, W. C. Barker, and R. E. Carson, "Count-rate dependent component-based normalization for the hrrt," *Nuclear Science, IEEE Transactions on*, vol. 54, pp. 486–495, 2007.